

## Inorganic–Organic Hybrid Materials Prepared from Zirconium Oxo-Clusters and 2-Hydroxyethyl Methacrylate

Fabrizio Girardi,<sup>1</sup> Luca Fambri,<sup>2,3</sup> Simona Maggini,<sup>1</sup> Rosa Di Maggio<sup>1,3</sup>

<sup>1</sup>Department of Civil, Environmental and Mechanical Engineering, University of Trento, 38123 Trento, Italy

<sup>2</sup>Department of Industrial Engineering, University of Trento, 38123 Trento, Italy

<sup>3</sup>Interuniversity National Consortium for Science and Technology of Materials (INSTM), 50121 Firenze, Italy

Correspondence to: F. Girardi (E-mail: fabrizio.girardi@unitn.it)

**ABSTRACT:** This article describes the preparation and characterization of hybrid materials obtained from the polymerization of vinyl-substituted zirconium oxo-clusters  $[\text{Zr}_6\text{O}_4(\text{OH})_4(\text{OOCCH}_2\text{CHCH}_2)_{12}(\text{n-PrOH})]_2 \cdot 4(\text{CH}_2\text{CHCH}_2\text{COOH})$  (Zr12) and 2-hydroxyethyl methacrylate (HEMA). The zirconium oxo-clusters serve as cross-linking agents, forming a 3D network by means of the copolymerization of their vinylic ligands with HEMA. To optimize the conditions for cross-linking, the polymerization was monitored with a differential scanning calorimeter. The resulting hybrid materials were also characterized using thermo-mechanical techniques. There was evidence not only of a greater rigidity above  $T_g$ , but also of a better thermal stability for several hybrid formulations than for simple poly-2-hydroxyethyl methacrylate. After immersion in water, the hybrids containing 20 or 60% w/w zirconium oxo-clusters also showed a stable behavior with an equilibrium swelling at about 27 and 18% w/w of water, respectively. © 2014 Wiley Periodicals, Inc. *J. Appl. Polym. Sci.* **2015**, *132*, 41568.

**KEYWORDS:** copolymers; glass transition; swelling; thermal properties

Received 9 June 2014; accepted 29 September 2014

DOI: 10.1002/app.41568

### INTRODUCTION

There has been intensive research on organic–inorganic hybrid materials in recent years, focusing on combining the properties of nano-sized inorganic moieties with those of organic polymers.<sup>1,2</sup> By comparison with pure organic polymers, hybrid materials show remarkable changes in their thermal and mechanical, and sometimes even magnetic properties. Poly(2-hydroxyethyl methacrylate) (PHEMA) is a particular example, being the first synthetic hydrogel to be used in biomedical and pharmaceutical applications.<sup>3</sup> PHEMA and PHEMA-based hydrogels are widely used for contact lenses, in controlled drug release systems,<sup>4,5</sup> sensors,<sup>6</sup> membranes,<sup>7</sup> and implant coatings to prevent bio-fouling.<sup>5,8–13</sup> Both ultraviolet radiation and thermal energy (infrared radiation) can initiate the polymerization reaction, depending on used photo- or thermal initiator. Many attempts to create hybrid PHEMA-based materials have aimed to change the water uptake by the polymer, which is swellable. The degree of swelling equilibrium depends on the material's thickness (in the case of coatings or membranes), the polymerization mechanism, and the amount and nature of the cross-linker used.<sup>14–16</sup> For instance, soaking PHEMA in drug solutions is still an inexpensive method for loading drugs in lenses or biomedical drug release devices.<sup>4,5</sup> More recently, there have

been studies on the use of nanofilms of PHEMA on the inner walls of microtubes to enhance boiling heat transfer at high heat fluxes in microreactors, or fuel cells.<sup>8</sup>

While the interest in PHEMA is prompted by its easy polymerization and useful physical properties (e.g., permeability of membranes to oxygen, mechanical and viscoelastic behavior, thermal, and dielectric properties),<sup>17</sup> the polymer's stiff, brittle nature in the dry state has some drawbacks.<sup>18</sup> Alongside the copolymerization of HEMA (2-hydroxyethyl methacrylate) with other types of monomer,<sup>19,20</sup> the most popular way to improve its mechanical and thermal properties is by introducing fillers, and particularly highly dispersed silicas.<sup>21,22</sup> In other words, the polymer's structure can be controlled by means of a polymerization in the presence of silica fillers. An inorganic oxide phase, such as  $\text{TiO}_2$ , has also been incorporated in PHEMA by graft/crosslink polymerization to make photoelectrodes for solar cells or photocatalysts for organic pollutant degradation.<sup>11–13</sup> PHEMA embedded  $\text{ZrO}_2$  was also investigated, using a one-step process that involved mixing zirconium alkoxide and HEMA with benzoyl peroxide (BPO).<sup>23–25</sup> The *in situ* formation of zirconium oxo-clusters was claimed to occur in this case. The mixtures containing BPO polymerized and stiffened within minutes after a mild thermal treatment, and the resulting hybrid

**Table I.** Selected DSC Data of Fresh Oxo-Cluster/HEMA Mixture (Initiator BPO 0.5%) at Different Content of Zr12 Crystals Polymerized During First DSC Scan

Oxo-crystal content (%)	Exothermal peak onset (°C)	Exothermal peak $T_{max}$ (°C)	Reaction enthalpy (J/g)	Mass loss after DSC (%)
0	110	123	314	4
2	108	120	364	4
4	112	121	357	5
6	108	122	351	4
10	119	125	348	2
20	112	122	341	1
30	108	121	309	3
60	112	123	232	2

materials were homogeneous and transparent, but brittle and not swellable.<sup>23–25</sup> To retain the hydrogel properties and toughness of PHEMA after hybridization, crystalline carboxylate-functionalized oxo-clusters with polymerizable functionalities have been used in free radical polymerization processes with HEMA monomer.<sup>26</sup> The current study focuses on investigating how hybrid zirconium oxo-clusters modify the properties of PHEMA and improve its thermal stability. The hybrid polymers were characterized with the aid of differential scanning calorimetry (DSC) and dynamic mechanical analysis (DMA) to show the type and extent of the interactions between the inorganic and organic moieties.

## EXPERIMENTAL

### Materials

Zirconium propoxide ( $Zr[OnPr]_4$ ) (70% w/w in propanol) was purchased from ABCR GmbH, Karlsruhe, Germany. Vinylacetic acid 97% (VAA), HEMA and BPO were purchased from Aldrich (Milan, Italy). All the chemicals were stored under argon to prevent the detrimental action of oxygen and moisture, and the solvents were additionally stored on molecular sieves.

Irgacure 819 [Phosphine oxide, phenylbis (2, 4, 6-trimethylbenzoyl)]—a kind gift from Ciba Speciality Chemicals (Switzerland) was used as photoinitiator at 4% w/w in HEMA solution.

### Zirconium Oxo-Cluster Synthesis

The zirconium oxo-cluster  $[Zr_6O_4(OH)_4(OOCCH_2CHCH_2)_{12}(n-PrOH)]_2 \cdot 4(CH_2CHCH_2COOH)$ , (Zr12), bearing 24 vinylacetate functionalities, was synthesized according to the procedure reported elsewhere.<sup>26,28</sup> VAA and zirconium *n*-propoxide were mixed in the molar ratio of 4 : 1 (with a little excess acid) and set aside until crystal precipitation took place. All operations for oxo-cluster synthesis were performed under argon using standard Schlenk techniques.

### Copolymerization of Zirconium Oxo-Cluster and HEMA via Thermal Polymerization

Hybrid bulk materials were obtained after polymerizing HEMA with different percentages of Zr12 (0–60%, as shown in Table I). To prepare the solution, the zirconium oxo-cluster Zr12 was dispersed in HEMA in a Schlenk tube and stirred. After the oxo-cluster had dissolved completely, BPO was added in proportions of 0.5% of HEMA. The resulting solutions were

placed in polypropylene tubes with an outer diameter of 4 mm and polymerized in an oven at 70°C for 3 h. As-polymerized samples were stored in a sealed container with silica gel desiccant. For comparison, some samples containing BPO in the extent of 4% w/w of HEMA were prepared at 50°C for 20 h.

Some samples were aged in air, at 25°C and 70% relative humidity for 6 months.

### Copolymerization of Zirconium Oxo-Cluster and HEMA Using Photopolymerization

Hybrid bulk materials were obtained after photopolymerizing HEMA with Zr12 in proportions of 10% w/w of HEMA monomer. The solution of the two reagents was stirred for 5 min before Irgacure 819 photoinitiator was added (4% w/w of the total weight of the monomer). After stirring for a further 15 min, the solution was photopolymerized in a teflon beaker (10 mL) under a UV lamp (Helios Italquartz S.r.l., 125W, 230V, emission range 250–450 nm) for 20 min (a time optimized in the light of time-resolved IR measurements). The distance between the lamp and the substrate was set to 20 cm.

### Sample Characterization

Infrared spectra were acquired with a FTIR spectrophotometer (Spectrum One, Perkin Elmer) in the range 4000–500  $cm^{-1}$  using an attenuated total reflectance attachment (resolution of 4  $cm^{-1}$ , 64 scans).

Differential scanning calorimetry (DSC) analyses were performed with a DSC92 Setaram in the range of 30–200°C with a heating rate of 10°C/min, flushing with nitrogen at 100 mL/min in accordance with ASTM E2160-04 (Reapproved 2012) “Standard Test Method for Heat of Reaction of Thermally Reactive Materials by Differential Scanning Calorimetry”.

Dynamic mechanical analysis (DMA) was performed using a Seiko DMS 6100 instrument in shear mode on at least three cured disks with an area of 12 mm<sup>2</sup> and a thickness of 3.5 mm. The shear storage ( $G'$ ) and loss ( $G''$ ) modulus, and the damping factor ( $\tan \delta$ ) were measured in two subsequent scans from 30 to 200°C, with a heating rate of 3°C/min at a frequency of 1 Hz, and with a dynamic displacement of five micron in the direction of the diameter. The  $T_g$  values were read off as the temperatures of the peak of loss modulus, in accordance with

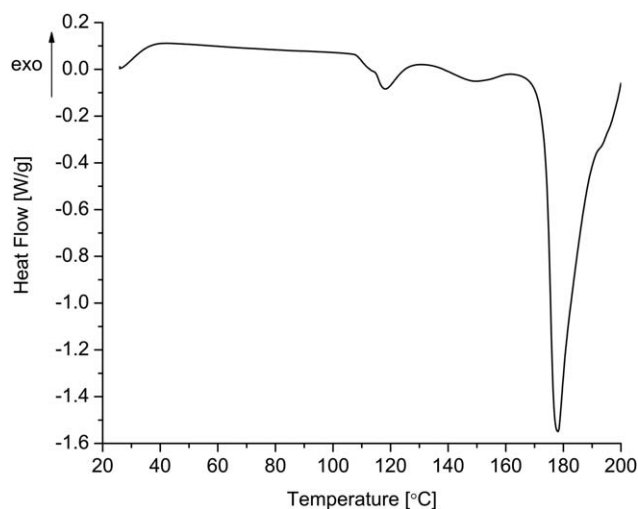


Figure 1. DSC analysis of Zr12 oxo-clusters (6 months after preparation).

ASTM E1640-13 “Standard Test Method for Assignment of the Glass Transition Temperature by Dynamic Mechanical Analysis”.

## RESULTS AND DISCUSSION

To obtain a PHEMA with a tailored hydrophilic behavior, the synthetic route involved copolymerizing organic monomers with preformed metal oxo-clusters, which are mono-dispersed structures having an inorganic core capped with organic ligands, even polymerizable. The preparation and characterization of organic–inorganic (I–O) hybrid materials obtained from the reaction of HEMA and zirconium vinylacetate oxo-clusters (Zr12), using a thermal initiator (BPO) or a photoinitiator (Irgacure 819), are presented below.

The preparation of such crystals and their reactivity have been described elsewhere.<sup>26–28</sup> The crystals’ elemental analysis (C, 36.74%; H, 4.14%; Zr, 25.20% w/w) suggests the following theoretical formula  $[\text{Zr}_6\text{O}_4(\text{OH})_4(\text{OOCCH}_2\text{CHCH}_2)_{12}(\text{n-PrOH})]_2 \cdot 4(\text{CH}_2\text{CHCH}_2\text{COOH})$ , so they are considered dimers of Zr12. The crystalline structure of the VAA-substituted zirconium oxo-cluster (not discussed in this study) was found consistent with the structure of Zr12 clusters described by Schubert et al.<sup>26,29–36</sup> According to previously-published results<sup>32</sup>, Zr12 can be described as dimers of Zr6 characterized by different arrangements of VAA ligands, which may be terminal, chelating or bridging. The two Zr6 clusters are linked by bridging carboxylate groups, and form the Zr12 cluster. The DSC curve of the crystals (Figure 1) shows two main endothermic peaks attributable to the evaporation of n-propanol ( $T = 113^\circ\text{C}$ ; 7.4 J/g) and VAA ( $T = 173^\circ\text{C}$ ; 88.5 J/g), respectively. The mass loss observed after DSC analysis was 21.9%, so that eight VAcOH and two PrOH molecules are supposed to be given off for each cluster.<sup>27</sup> These oxo-clusters of crystals were found stable after 6 months of storage, as documented by the DSC profile and the mass loss. The material recovered after the DSC scan at  $200^\circ\text{C}$  was brittle. FT-IR measurements performed before and after DSC [Figure 2(a,b), respectively] show that a rearrangement toward the enolic form (peak of  $\nu_{\text{C}=\text{C}}$  at  $1638\text{ cm}^{-1}$ ) occurred during heating.

Zr12 crystals are colorless and do not dissolve in water, but they are soluble in various organic solvents, such as toluene, Tetrahydrofuran (THF), and ethyl acetate. The four free acids are connected to the clusters by hydrogen bonds. The crystals do not swell in water.

It is worth noting that the solution of Zr12 crystals and BPO in THF showed a large exothermal peak of 240 J/g on DSC, centred at  $154^\circ\text{C}$ , and with a significant shoulder at  $175^\circ\text{C}$ .<sup>27</sup> This means that the vinyl groups are able to polymerize over a wide temperature range as a consequence of the variable availability for radical polymerization of the VAA ligands, which have different arrangements in the Zr12 structure. On the other hand, plain VAA cannot thermally polymerize in the liquid state with 4% BPO because of its evaporation, but it can react as an anchored ligand of an inorganic support. A similar effect has already been seen in other vinyl compounds, such as vinyl-trimethoxy silane, which polymerizes in the presence of even small amounts of Zr12.<sup>27</sup>

Bulk hybrid materials were obtained after polymerizing HEMA with different w/w proportions of Zr12 and BPO. The polymerization was monitored using DSC to optimize the conditions for cross-linking and exothermal polymerization peaks were identified from the DSC data on the hybrid polymers.

The HEMA monomers polymerization temperature seems to be scarcely affected by the presence of Zr12 up to a content of 10% w/w [see Table I and Figure 3(a)]; on the other hand, its main effect is to increase the polymerization enthalpy of the HEMA [see Figure 3(b)]. When the crystal content is increased to 30 and 60% (see Figure 4), however, the polymerization onset temperature increases and the area of the polymerization peak decreases, as already seen in Figure 3(b); and the higher the crystal content, the lower the optical transparency: the polymerized samples appeared increasingly opaque and whitish beyond 20% w/w. The most interesting result observable in Figure 4, however, is that a peak at higher temperature appears when the crystal content is higher. In fact, the inset in the same figure shows exothermal shoulders at about  $155^\circ\text{C}$ , attributable to polymerization involving the vinyl groups of Zr12, as

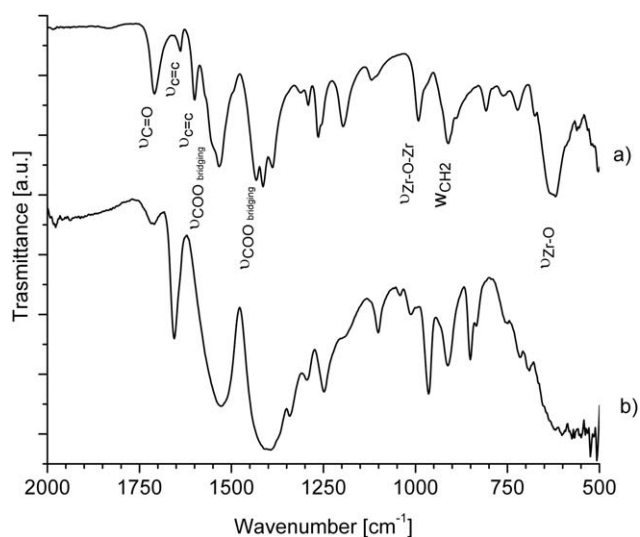
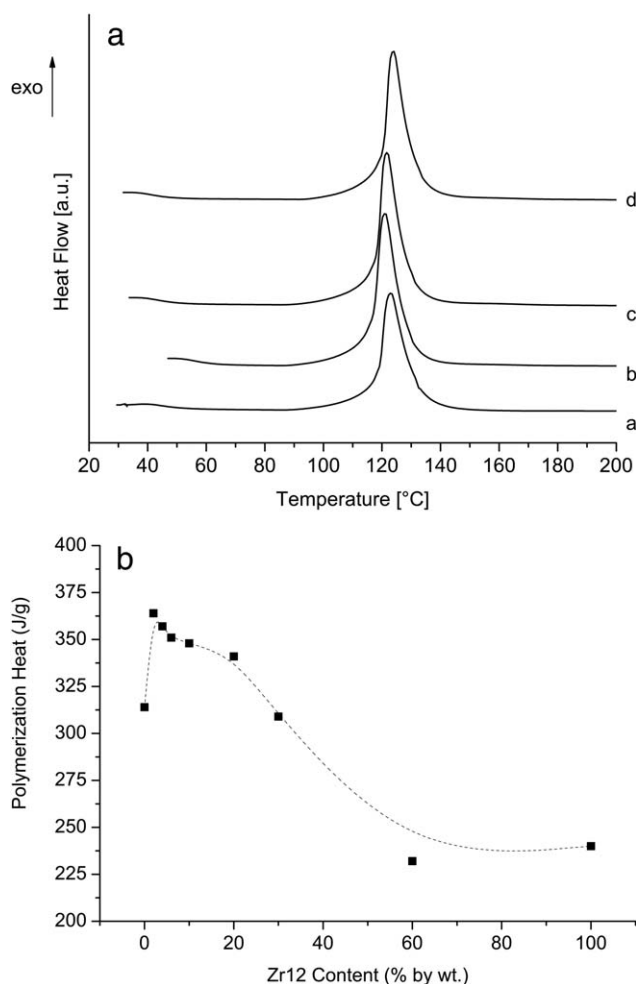
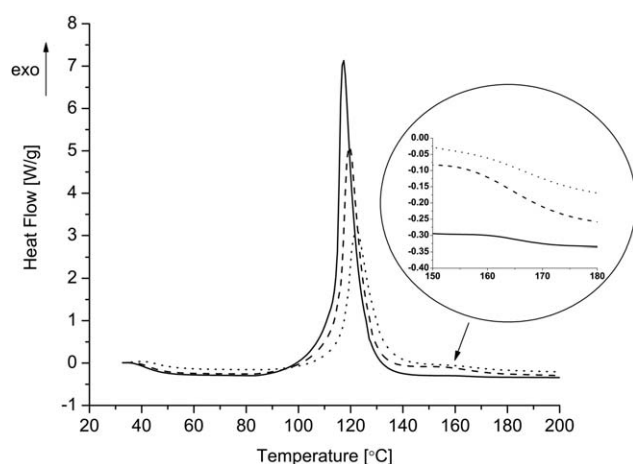


Figure 2. FT-IR spectra of Zr12 before (a) and after (b) DSC analysis.



**Figure 3.** (a) DSC curves of Zr12/HEMA and BPO (0.5% w/w) with a different amount of crystal: 0% (a), 2% (b), 6% (c), 10% w/w (d). (b) Polymerization enthalpy of the Zr12/HEMA hybrids (BPO at 0.5% w/w) vs. crystal content. See details of polymerization of Zr12 crystals in Ref. 27.



**Figure 4.** DSC curves of the Zr12/HEMA and BPO (0.5% w/w) with different amounts of crystal: 0% (solid line), 30% (dashed line), 60% w/w (dotted line).

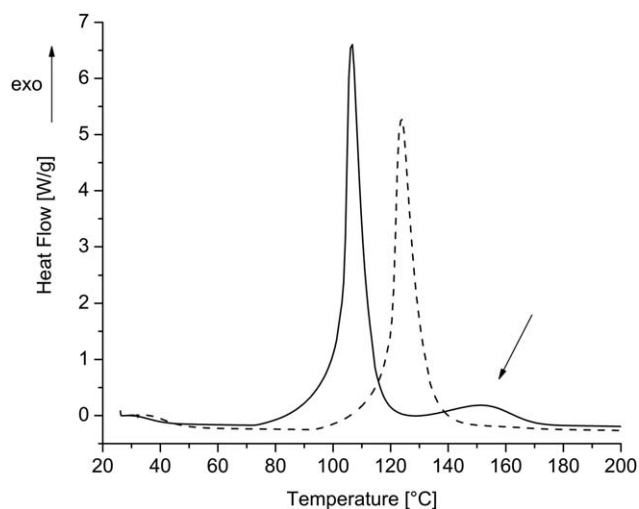


**Figure 5.** DSC curves of the system prepared with HEMA, 10% w/w of crystals and a different amount of BPO: 4% (solid line), 0.5% w/w (dashed line). The arrow indicates the extra exothermal polymerization involving vinyl groups of Zr12 oxo-cluster.

previously reported in the literature.<sup>27</sup> The higher the proportion of crystals, the greater the heat evolved. To shed light on the contribution of Zr12 to the whole polymerization process, BPO was increased to 4% w/w and Figure 5 shows the DSC curves for two samples, both containing 10% w/w of crystals, but different percentages of BPO. The increase of BPO coincided with a decrease in onset temperature of the polymerization peak. The Figure 5 also shows a remarkable exothermal polymerization at about 155°C already with 10% w/w of Zr12 oxo-cluster (see Figure 5). As discussed earlier, this higher temperature process can be attributed to cross-linking between the residual monomer and the vinyl ligands bonded to zirconium oxo-clusters. It is worth noting that this secondary peak increases with BPO content: the higher the amount of radical initiator, the greater the cross-linking.

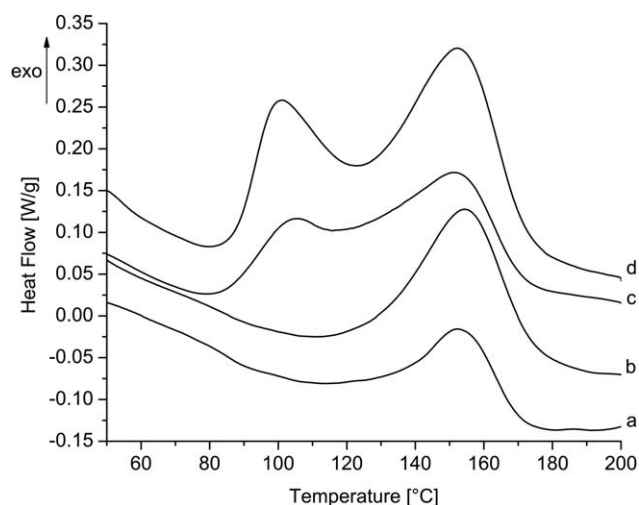


**Figure 6.** DSC curves of hybrid materials polymerized with 4% w/w of BPO at 50°C for 20 h and percentage of crystals 2% (a), 6% (b), 10% (c), 20% (d), respectively.



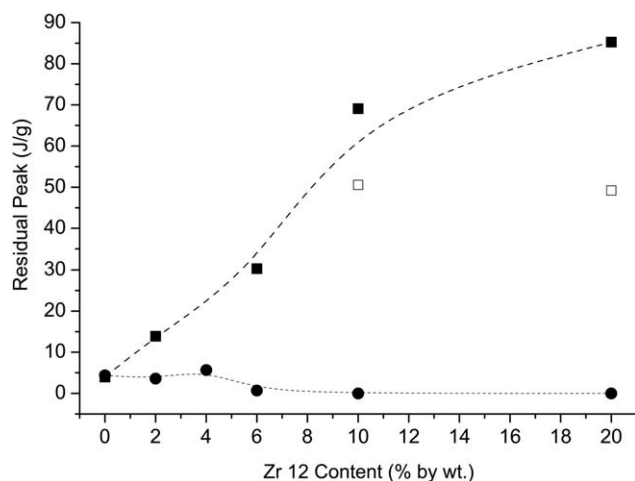


**Figure 7.** Total polymerization heat vs. Zr12 content, calculated under the residual peaks of the hybrid samples polymerized with 0.5% w/w BPO at 70°C for 3 h (●) and polymerized with 4% w/w of BPO at 50°C for 20 h (■). The residual heat of polymerization of peak at high temperature of samples with 10 and 20% of crystals and polymerized at 50°C, were calculated as partial integral from Figure 6 and reported (□).

The curves of all the samples polymerized with 4% of BPO at 50°C for 20 h (Figure 6) show peaks at about 150°C, attributable to a residual polymerization involving the vinyl groups of

Zr12. The DSC curves of the samples with the highest content of Zr12 crystals (10 and 20%) evidenced a second peak, at lower temperature, and it is attributable to the residual polymerization of HEMA. The large amount of clusters seems to hinder the radical polymerization at 50°C even with 4% of initiator. The total enthalpy of residual polymerization increased proportionally with the percentage of crystals, as shown in Figure 7. The presence of residual peaks (one or two depending on the amount of Zr12 crystals used) suggests that the curing in oven was not completed at 50°C for 20 h. On the other hand, the peaks of residual polymerization of samples prepared at 70°C with 0.5% of BPO were negligible.

The results of DMA show that the aging affects in different extent the specimens. Figure 8(a) compares the damping factor ( $\tan \delta$ ) of the first heating cycle of fresh specimens polymerized with 0.5% of BPO at 70°C for 3 h: the onset and peak temperatures of the hybrids were considerably lower than those of plain PHEMA, while the mass losses were negligible. Aging in air induced a moisture uptake. In fact the mass loss during first scan was about 5% w/w and seemed to be inversely proportional to the quantity of crystals, consistently with the mass loss recorded during the DSC analyses. Moreover the  $\tan \delta$  peak shows a shoulder at 80–90°C [Figure 8(b)]. This is related to the fraction of PHEMA that absorbed moisture, whereas the peak at about 120°C coincides with the glass transition

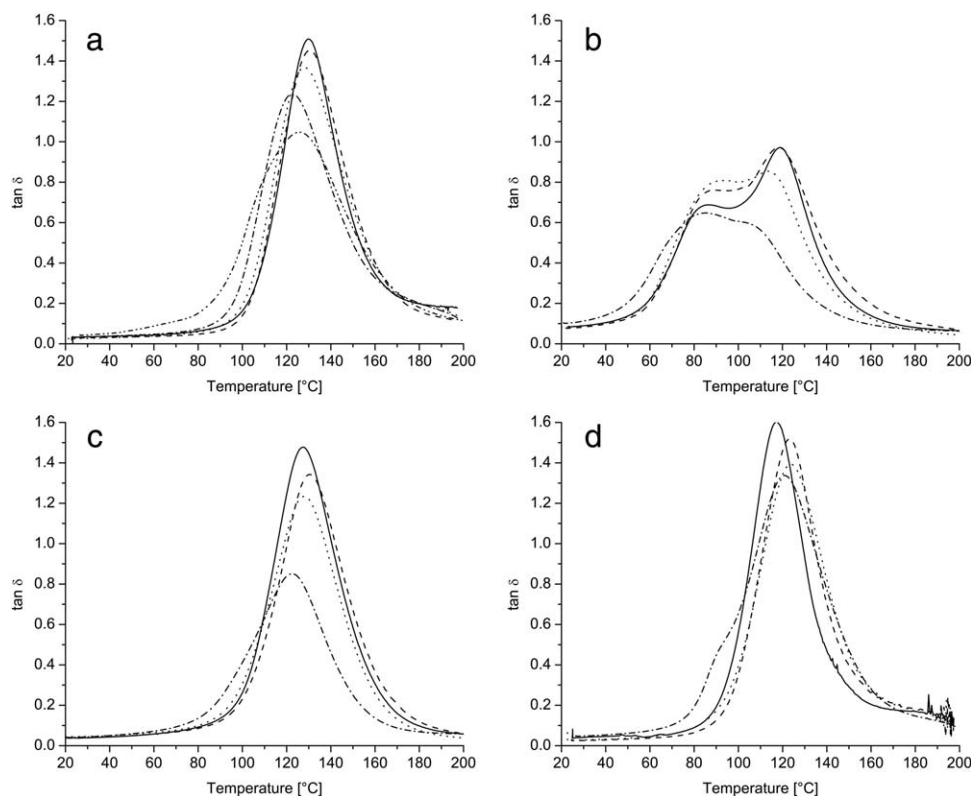


**Figure 8.** (a) Damping factor ( $\tan \delta$ ) of PHEMA (—) and hybrids polymerized with 0.5% w/w of BPO at 70°C for 3 h (first scan). Crystal content of 2% (---), 6% (....), 10% (-.-.-), and 20% (-.-.-.-). (b) Damping factor ( $\tan \delta$ ) after 6 months of PHEMA (—) and hybrids polymerized with 0.5% w/w of BPO at 70°C for 3 h (first scan). Crystal content of 2% (---), 6% (....), and 10% (-.-.-). (c) Damping factor ( $\tan \delta$ ) after 6 months of PHEMA (—) and hybrids polymerized with 0.5% w/w of BPO at 70°C for 3 h (second scan). Crystal content of 2% (---), 6% (....), and 10% (-.-.-). (d) Damping factor ( $\tan \delta$ ) of PHEMA (—) and hybrids polymerized with 4% of BPO at 50°C for 20 h (first scan). Crystal content of 2% (---), 6% (....), and 20% (-.-.-).

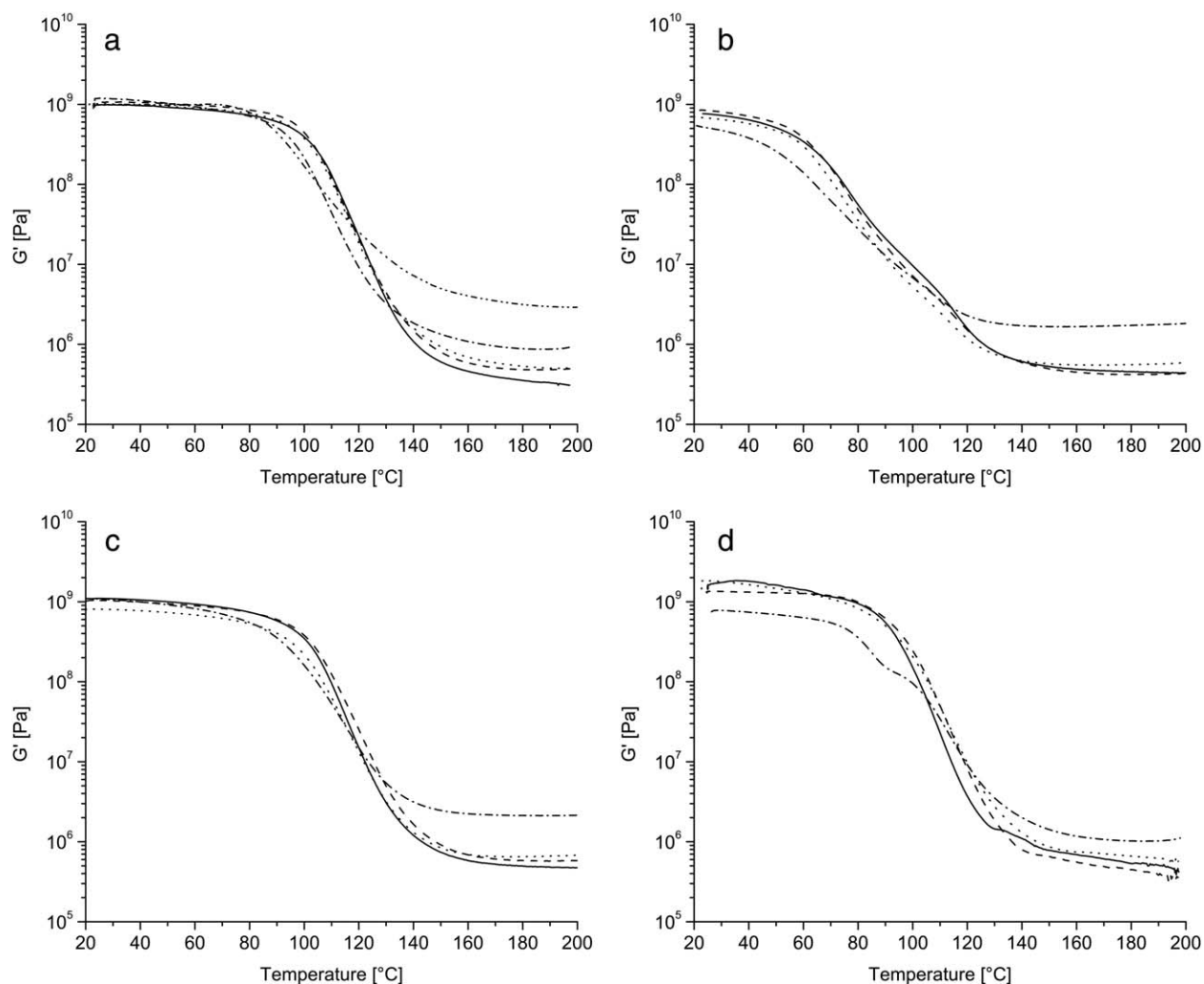


**Figure 9.** (a) Storage modulus ( $G'$ ) of PHEMA (—) and hybrids polymerized with 0.5% w/w of BPO at 70°C for 3 h (first scan). Crystal content of 2% (---), 6% (....), 10% (-.-.-), and 20% (-.-.-). (b) Storage modulus ( $G'$ ) after 6 months of PHEMA (—) and hybrids polymerized with 0.5% w/w of BPO at 70°C for 3 h (first scan). Crystal content of 2% (---), 6% (....), and 10% (-.-.-). (c) Storage modulus ( $G'$ ) after 6 months of PHEMA (—) and hybrids polymerized with 0.5% w/w of BPO at 70°C for 3 h (second scan). Crystal content of 2% (---), 6% (....), and 10% (-.-.-). (d) Storage modulus ( $G'$ ) of PHEMA (—) and hybrids polymerized with 4% w/w of BPO at 50°C for 20 h (first scan). Crystal content of 2% (---), 6% (....), and 20% (-.-.-).

temperature ( $T_g$ ) of the dry fraction. When a second heating cycle was performed on the same aged samples [Figure 8(c)], the curves overlapped quite well with that of the as-polymerized ones and only one peak in the  $\tan \delta$  curve was apparent, albeit shifted to a higher temperature. The mass loss measured after the second scan was of the order of 0.4–0.6% w/w and this also confirms that aging in air allows moisture to be absorbed.

The first DMA scan of the specimens polymerized at 50°C with 4% of BPO for 20 h showed a single peak curve [Figure 8(d)], with a small shoulder at about 90°C for hybrids at 20% of crystals, in correspondence to the first exothermal residual peak shown in Figure 6. Moreover it should be underlined that the peak temperature of hybrids was higher than plain PHEMA, 125–130°C with respect to 120°C.

Figure 9(a–d) show the dynamic shear moduli vs. temperature of all the same specimens, mentioned before. The presence of

Zr12 induces an increase of stiffness especially above  $T_g$ . In fact, hybrids in this zone showed a higher storage modulus  $G'$  than PHEMA. The organic chains were shorter in the presence of crystals, which hindered the organic polymer chains' growth. The greater the crystal content, the lower the  $T_g$ . A decrease in the number of hydrogen bonds may also account for the lower  $T_g$  and modulus, since they contribute significantly to the properties of PHEMA. The fresh samples exhibited both a higher conservative modulus and a higher  $T_g$  than the aged samples [Figures 8(a,b) and 9(a,b)], because of the moisture uptake discussed before. Accordingly, an increase of both modulus and  $T_g$  of the aged samples was evident in the second heating cycle [Figures 8(c) and 9(c)].

Figure 9(d) shows the shear storage modulus of the samples polymerized at 50°C with 4% w/w of BPO. It can be noted that hybrids containing 20% of crystals evidenced not only a lower

**Table II.** Glass Transition Temperature ( $T_g$ ), Shear Storage Modulus ( $G'$ ) and Cross-Linking Factor  $C$  of HB-10 (PHEMA with 10% w/w of Zirconium Oxo-Cluster and 0.5% w/w of BPO), HI-10 (PHEMA with 10% w/w of Zirconium Oxo-Cluster and 3% w/w IRGACURE 819), PHEMA(I) (3% w/w of IRGACURE 819), and PHEMA(B) (0.5% w/w of BPO)

	$T_g^a$ (°C)		$G'^b$ below/above $T_g$ (MPa)		Cross-linking factor $C$	
	1st scan	2nd scan	1st scan	2nd scan	1st scan	2nd scan
HB-10	70	90	465/1.7	1053/2.1	0.37	0.20
HI-10	99	115	311/0.2	138/1.1	0.06	0.80
PHEMA(I)	81	92	562/0.6	631/0.6	0.11	0.09
PHEMA(B)	99	102	758/0.5	1101/0.5	0.06	0.04

<sup>a</sup>Glass transition temperature ( $T_g$ ) was measured at the maximum point on the loss modulus peak.

<sup>b</sup>Shear storage modulus ( $G'$ ) measured at 40 and 160°C.

modulus, but also a decreasing step between 80 and 100°C, in conformity to the shoulder in tan delta peak [Figure 8(d)]. Moreover PHEMA and other hybrids (with 2 and 6% of crystal content) show below  $T_g$  a higher modulus than the samples polymerized with 0.5% w/w of BPO.

Some samples were also prepared using photopolymerization with Irgacure (HI) to compare their properties with those of the hybrids obtained by thermal polymerization with BPO (HB) (4% w/w of both initiators) and the same oxo-cluster content, i.e., 10% w/w of Zr12 (Table II). The peak of residual polymerization of the photo-polymerized samples was characterized by a low onset temperature, at about 80°C and 11.4 J/g. The most important difference between the two types of material concerns their mechanical behavior (Table II). The damping factor, shear storage, and loss moduli of the aged samples prepared by UV photopolymerization—recorded vs. temperature during the first and second scans—are shown in Figure 10(a,b). Unlike the aged samples containing the same amount of Zr12 (10% w/w) polymerized by means of a thermal treatment, they appear constant up to  $T_g$ , although the shear storage moduli of the photopolymerized samples show lower values at lower temperatures. The  $T_g$  of the sample polymerized by means of a thermal treatment, measured as the temperature of the maximum loss modulus  $G''$ , was 70 and 90°C in the first and second scans, respectively, as opposed to 99 and 115°C for the photopolymerized sample. The  $T_g$  and shear storage modulus of the two samples are shown in Table II, along with the cross-linking factor ( $C$ ).

The cross-linking factor ( $C$ ) is a modification of the transition intensity factor reported by Diez-Gutierrez et al.,<sup>36</sup> according to the equation.

$$C = \frac{G'_a}{G'_b - G'_a} \times 100$$

where  $G'_b$  and  $G'_a$  denote the storage moduli below and above the glass transition temperature, i.e., at 40 and 160°C, respectively. The values of  $C$  confirm that the presence of zirconium oxo-clusters contributes to improving the rigidity of the polymer beyond the glass transition. Photopolymerization appears to be less efficient than thermal polymerization in inducing cross-linking in the presence of zirconium oxo-clusters. At this regard all the DMA results confirmed that the conditions of

polymerization and curing (especially the amount and type of initiator) are really important to determine the final characteristics and properties of fresh and aged hybrid.

Finally, the water absorption of selected hybrid polymers, all polymerized at 70°C, was measured in distilled water at 25°C, monitoring their relative weight variation for 14 days. The

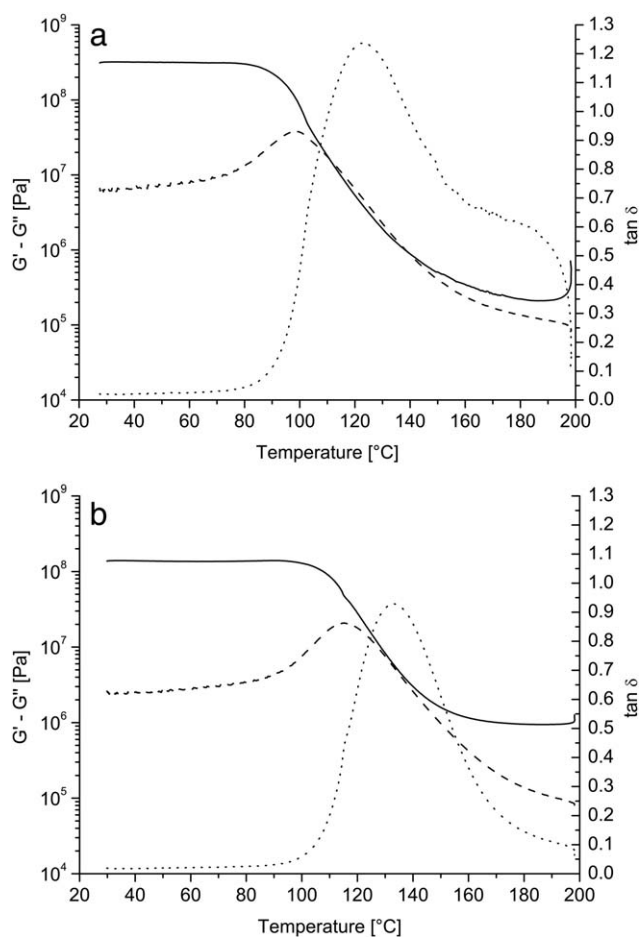


**Figure 10.** Storage modulus  $G'$  (—), loss ( $G''$ ) (---) modulus, and  $\tan \delta$  (····) of the aged samples (10% w/w of crystal) prepared by UV photopolymerization (first scan). (b) Storage modulus  $G'$  (—), loss ( $G''$ ) (---) modulus, and  $\tan \delta$  (····) of the aged samples (10% w/w of crystal) prepared by UV photopolymerization (second scan).

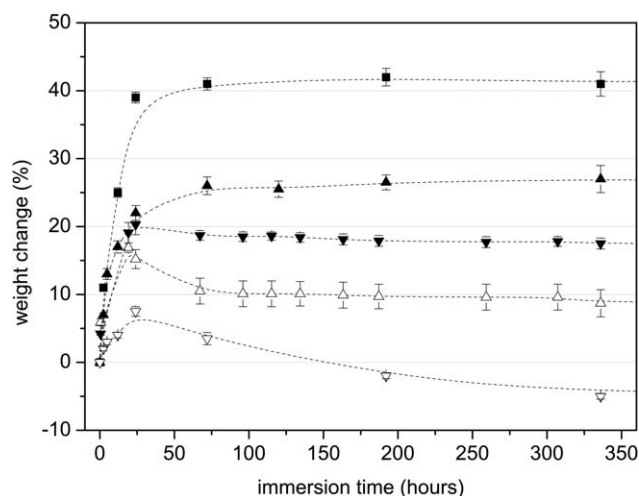


**Figure 11.** Effect of weight change after immersion in water at 25°C for 14 days: Comparison of pure poly-2-hydroxyethyl-methacrylate (■), co-polymerized with Zr12 at 20 (▲), 60 (▼)% w/w and co-polymerized with comparable amounts of zirconium *n*-propoxide (Zr : HEMA = 1 : 10 (△) and Zr : HEMA = 1 : 4 (▽)).<sup>23–25</sup>

absorption of the samples containing preformed Zr12 crystals were compared with that of samples containing comparable HEMA/Zr molar ratios from 10 : 1 to 4 : 1, but prepared by a mixture of HEMA and zirconium *n*-propoxide.<sup>23</sup> This latter preparation was claimed to bring about *in situ* formed zirconium oxo-clusters by the reaction of HEMA and zirconium *n*-propoxide before polymerization and able to cross-link HEMA in a effective way.<sup>23–25</sup>

All samples exhibited a high rate of absorption in the first 24 h, the highest value being recorded for pure PHEMA, as expected and shown Figure 11. The hybrids with *in situ* formed oxo-clusters<sup>23–25</sup> showed different water absorption from that of plain PHEMA and the samples with 20 and 60% w/w of pre-formed Zr12 oxo-clusters. The latter showed a hydrophilic behavior, with an almost constant equilibrium adsorption of about 27 and 18% w/w, respectively — i.e., lower than in PHEMA (42% w/w). The weight gain seems to be proportional to the crystal content, but we have to bear in mind that with up to 20% w/w of crystals the hybrids are still transparent, whereas they become more and more opaque and whitish beyond said limit. On the other hand, the hybrid samples with *in situ* formed zirconium oxo-clusters were rigid and transparent. Whatever the inorganic moiety, they exhibited hydrolytic instability and significant mass loss already after 48 h of immersion. Accordingly, the hybrid polymers with *in situ* formed zirconium oxo-clusters show a completely different thermo-mechanical behavior. The sample prepared in this way showed a  $T_g$  at about 80°C in the first scan and above 150°C in the second one, along with an increase in the storage modulus due to cross-linking.<sup>23–25</sup>

## CONCLUSIONS

Zirconium oxo-clusters, prepared by reaction of zirconium *n*-propoxide and acid vinylacetic, interacted through condensation with HEMA, giving rise to a stable solution. In the presence of either thermally or photoinitiator of polymerization, the solu-

tion changes into a solid material, evolving an amount of reaction heat that depends on the proportion of oxo-clusters. The vinyl groups capping the organic zirconia core of the oxo-clusters are demonstrated to be involved in copolymerization with HEMA at higher temperature than that of the plain organic monomer. In fact, calorimetric analyses showed a high-temperature exothermic peak attributable to the cross-linking/polymerization of residual vinyl groups. Both the temperature and the intensity of this peak increased with the amount of zirconium oxo-cluster in the hybrid materials.

The Zr12/PHEMA materials exhibited a higher storage modulus than plain PHEMA above  $T_g$ . For all samples, there was a marked increase in rigidity beyond the glass transition phase, which can be explained by the occurrence of cross-linking. This depends strictly on the type of initiator and the polymerization conditions. In this regard, a thermal post-treatment is beneficial for UV-cured samples.

The Zr12/PHEMA materials showed a different swelling behavior in water from that of the pure polymer, and a greater hydrolytic stability than in the hybrid systems polymerized by directly mixing HEMA and zirconium *n*-propoxide.

In conclusion, Zr12 can be used successfully to prepare hybrid materials based on zirconium derivatives and PHEMA, particularly for the purpose of tailoring its properties and behavior in both wet and dry states. All the results confirm that the conditions of preparation, polymerization, and curing are crucial to determine the final characteristics and properties of fresh and aged hybrids.

## ACKNOWLEDGMENTS

The Provincia Autonoma di Trento (PAT) and the “CENACOLI” project are acknowledged for partly funding the research.

## REFERENCES

- Ishiwata, T.; Furukawa, Y.; Sugikawa, K.; Kokado, K.; Sada, K. *J. Am. Chem. Soc.* **2013**, *135*, 5427.
- Mosby, B. M.; Díaz, A.; Bakhmutov, V.; Clearfield, A. *ACS Appl. Mater. Interfaces* **2014**, *6*, 585.
- Wichterle, O.; Lim, D. *Nature* **1960**, *185*, 117.
- Paradiso, P.; Galante, R.; Santos, L.; Alves de Matos, A. P.; Colaco, R.; Serro, A. P.; Saramago, B. *J. Biomed. Mater. Res. B* **2014**, *102*, 1170.
- Zamfir, M.; Rodriguez-Emmenegger, C.; Bauer, S.; Barner, L.; Rosenhahn, A.; Barner-Kowollik, C. *J. Mater. Chem. B* **2013**, *1*, 6027.
- Baek, C.-H.; Moon, B.-C.; Lee, W.-E.; Kwak, G. *Polym. Bull.* **2013**, *70*, 71.
- Cömert, Ş. C.; Odabaşı, M. *Mater. Sci. Eng. C* **2014**, *34*, 1.
- Kaya, A.; Demiryürek, R.; Armğan, E.; Ince, G.; Sezen, M.; Koşar, A. *J. Micromech. Microeng.* **2013**, *23*, 115017.
- Bach, L. G.; Rafiqul Islam, M.; Seo, S. Y.; Lim, K. T. *J. Appl. Polym. Sci.* **2013**, *127*, 261.
- Bolbukh, Y.; Tertykh, V.; Klonos, P.; Pissis, P. *J. Therm. Anal. Calorim.* **2012**, *108*, 1111.



11. Park, J. T.; Koh, J. H.; Seo, J. A.; Kim, J. H. *J. Mater. Chem.* **2011**, *21*, 17872.
12. Mesnage, A.; Abdel Magied, M.; Simon, P.; Herlin-Boime, N.; Jégou, P.; Deniau, G.; Palacin, S. *J. Mater. Sci.* **2011**, *46*, 6332.
13. De Giglio, E.; Cafagna, D.; Giangregorio, M. M.; Domingos, M.; Mattioli-Belmonte, M.; Comet, S. *J. Bioact. Compat. Pol.* **2011**, *26*, 420.
14. Davis, T. P.; Huglin, M. B. *Angew. Makromol. Chem.* **1991**, *189*, 195.
15. Garcia, O.; Blanco, M. D.; Gomez, C.; Teijon, J. M. *Polym. Bull.* **1997**, *38*, 55.
16. Mabileau, G.; Stancu, I. C.; Honoré, T.; Legeay, G.; Cincu, C.; Baslé, M. F.; Chappard, D. *J. Biomed. Mater. Res. A* **2006**, *77*, 35.
17. Montheard, J. P.; Chatzopoulos, M.; Chappard, D. *J. Macromol. Sci. Rev. Macromol. Chem. Phys.* **1992**, *32*, 1.
18. Bajpai, A. K.; Shrivastava, M. *J. Biomat. Sci-Polym. Ed.* **2002**, *13*, 237.
19. Arica, M. Y. *J. Appl. Polym. Sci.* **2000**, *77*, 2000.
20. Sahoo, S. K.; Prusty, A. K. *Int. J. Pharm. Appl. Sci.* **2010**, *1*, 1.
21. Samaržija-Jovanović, S.; Jovanović, V.; Konstantinović, S.; Marković, G.; Marinović-Cincović, M. *J. Therm. Anal. Calorim.* **2011**, *104*, 1159.
22. Alvarez, V. A.; Pérez, C. J. *J. Therm. Anal. Calorim.* **2012**, *107*, 633.
23. Di Maggio, R.; Fambri, L.; Guerriero, A. *Chem. Mater.* **1998**, *10*, 1777.
24. Di Maggio, R.; Fambri, L.; Mustarelli, P.; Camprostrini, R. *Polymer* **2003**, *44*, 7311.
25. Di Maggio, R.; Fambri, L.; Cesconi, M.; Vaona, W. *Macromolecules* **2002**, *35*, 5342.
26. Girardi, F.; Graziola, F.; Aldighieri, P.; Fedrizzi, L.; Gross, S.; Di Maggio, R. *Prog. Org. Coat.* **2008**, *62*, 376.
27. Di Maggio, R.; Dire, S.; Callone, E.; Girardi, F.; Kickelbick, G. *Polymer* **2010**, *51*, 832.
28. Di Maggio, R.; Dirè, S.; Callone, E.; Girardi, F.; Kickelbick, G. *J. Sol-Gel Sci. Techn.* **2008**, *48*, 168.
29. Puchberger, M.; Kogler, F. R.; Jupa, M.; Gross, S.; Fric, H.; Kickelbick, G.; Schubert, U. *Eur. J. Inorg. Chem.* **2006**, *16*, 3283.
30. Gao, Y.; Kogler, F. R.; Schubert, U. *J. Polym. Sci. Pol. Chem.* **2005**, *43*, 6586.
31. Kogler, F. R.; Koch, T.; Peterlink, H.; Seidler, S.; Schubert, U. *J. Polym. Sci. Pol. Phys.* **2007**, *45*, 2215.
32. Kogler, F. R.; Schubert, U. *Polymer* **2007**, *48*, 4990.
33. Kogler, F. R.; Jupa, M.; Puchberger, M.; Schubert, U. *J. Mater. Chem.* **2004**, *14*, 3133.
34. Schubert, U. *J. Sol-Gel Sci. Techn.* **2003**, *26*, 47.
35. Schubert, U. *J. Sol-Gel Sci. Techn.* **2004**, *31*, 19.
36. Diez-Gutierrez, S.; Rodriguez-Perez, M. A.; De Saja, J. A.; Velasco, J. I. *Polymer* **1999**, *40*, 5345.